

# Pressure Effects on Polymer Coil–Globule Transitions near an LCST

David S. Simmons and Isaac C. Sanchez\*

Department of Chemical Engineering, The University of Texas at Austin, 1 University Station C0400, Austin, Texas 78712-0231

Received July 9, 2009; Revised Manuscript Received November 23, 2009

**ABSTRACT:** A model for the pressure–temperature behavior of the coil–globule transition (CGT) of a polymer in dilute solution is developed without adjustable parameters. The predicted pressure–temperature conformational behavior semiquantitatively correlates with extant experimental data. The model yields a heating induced coil-to-globule transition (HCGT) temperature that increases with pressure until it merges with a cooling induced coil-to-globule transition (CCGT). The point at which the CCGT and HCGT meet is a hypercritical point that also corresponds to a merging of lower critical solution temperature (LCST) and upper critical solution temperatures (UCST). Theoretical results are discussed in terms of a generalized polymer/solvent phase diagram that possesses two hypercritical points.

## 1. Introduction

In a previous study, a new theory for the thermally (heating) induced coil-to-globule transition (HCGT) of an isolated polymer chain was presented.<sup>1</sup> The present study employs this model to investigate the pressure–temperature ( $P$ – $T$ ) behavior of the single chain coil–globule transition (CGT). The predicted single chain conformational transitions are widely understood to correspond to solution phase transitions. A central focus of this study will therefore be comparison with a recently proposed master curve describing polymer phase behavior,<sup>2</sup> shown qualitatively in Figure 1.

The polymer phase master curve is the result of recent work positing that the several classes of phase behavior delineated by Konyenburg and Scott<sup>3</sup> can be condensed into one master class for most polymer systems.<sup>2</sup> As shown schematically in Figure 1, this class is characterized by a single curve in  $P$ – $T$  space in which two UCST segments meet an intermediate LCST segment at hypercritical points labeled  $P_{min}$  and  $P_{max}$ . Since the present model does not exhibit a low temperature UCST,<sup>1</sup> this study will focus on behavior at temperatures significantly above that of  $P_{min}$ . In this temperature range, the LCST curve exhibits positive slope but is believed to curve over toward a maximum and a high-temperature UCST.

While such a maximum in polymer  $P$ – $T$  behavior has yet to be observed in polymer systems due to degradation,<sup>4,5</sup> several pieces of evidence point to its existence. From a theoretical standpoint, the possibility of a high temperature closed immiscibility loop has been shown based on the Sanchez–Lacombe (S–L) lattice fluid model.<sup>6</sup> On the experimental side, results in polymer–solvent systems have exhibited distinct negative curvature in the LCST, indicating the possibility of a maximum.<sup>4,7</sup> In addition, the phase lines of several small molecule systems<sup>8</sup> as well as systems of hydrocarbons in CO<sub>2</sub><sup>9</sup> have been experimentally shown to exhibit a maximum in pressure. Most convincingly, simulation<sup>10,11</sup> and experimental<sup>12</sup> studies of oligomers in supercritical solvents have provided evidence for a cooling induced coil-to-globule transition (CCGT) at temperatures above the HCGT, a phenomenon that

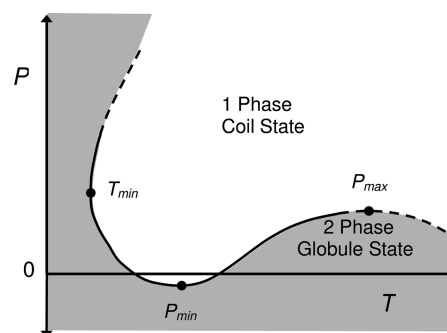


**Figure 1.** Schematic master curve of polymer solution phase<sup>2</sup> and conformational behavior. The grayed region denotes conditions under which a semidilute polymer/solvent mixture will be phase separated and in which the dilute phase will consist of polymer globules in dilute solution. The white region denotes conditions under which a polymer/solvent mixture will exist as a single phase that in the dilute limit will consist of single polymer coils in dilute solution. Dashed lines indicate phase boundaries lacking definitive experimental confirmation. The model presented here is restricted to temperatures above  $P_{min}$ .

would seem to require the presence of a maximum in the  $P$ – $T$  phase behavior.

Aside from the qualitative comparison outlined above, several quantitative measures of the  $P$ – $T$  behavior are of particular value for comparison with the literature and in technological applications. One such measure is quantitative prediction of the HCGT region of Figure 1, for which experimental data is available for a number of systems.<sup>4,13–16</sup> Alternatively, a common one parameter assessment of the  $P$ – $T$  behavior of interest in the literature is  $\partial T/\partial P$  of the CGT (or LCST) at zero pressure, also available for various systems. Final values of interest are the temperature and pressure of  $P_{max}$ . Identification of this point would facilitate a search for systems allowing experimental access to the high temperature UCST/cooling induced coil-to-globule transition (CCGT).

The present approach may also serve as a first step toward an expanded model that could quantitatively address the  $P$ – $T$  behavior of an isolated polymer chain in aqueous systems. The  $P$ – $T$  behaviors of the LCST and HCGT in aqueous solutions are of particular interest in recent literature,<sup>17–21</sup> largely because of

\*Corresponding author. E-mail: Sanchez@che.utexas.edu. Telephone: (512) 471-1020. Fax: (512) 475-7824.

their importance in smart polymers and biological applications.<sup>22–26</sup> For example, numerous studies have documented high pressure denaturation or conformational changes in proteins<sup>27–29</sup> that might be elucidated via the study of pressure induced chain collapse. Furthermore, coil–globule transitions have been identified in DNA.<sup>30–34</sup> Thus, a final objective of this study is to provide a prediction of the gyration radius or occupied volume fraction of an isolated chain as a function of pressure near the CGT. This may have long-term implications on the understanding of pressure induced conformational changes in biomolecules and synthetic chains at low concentrations.

The overall aim of this study is thus investigation of the  $P$ – $T$  behavior of the polymer CGT, as well as of the pressure induced coil–globule transition. This problem is approached via combination of the recent model for the thermally induced CGT of an isolated chain<sup>1</sup> with the S–L equation of state for the solvent. Limiting behavior in the case of infinite chain length is established, offering an analytical expression for the  $P$ – $T$  behavior of the CGT for a long chain. Additionally, numerical solutions are obtained for chains of finite length.

## 2. Theory

**2.1. Review of Coil–Globule Transition (CGT) Model.** In a recent paper, the present authors proposed a model for the thermally induced coil-to-globule transition (HCGT) of an isolated polymer chain. Within this model, the transition temperature  $\Theta$  is given by

$$(T_p^*/\Theta)\langle\phi\rangle_0 + [\ln(1-\phi_0) + \phi_0]/\phi_0 = 0 \quad (1)$$

where  $T_p^*$  is a characteristic temperature of the polymer,  $\langle\phi\rangle$  is the mean volume fraction occupied by the chain within its pervaded volume, “0” subscripts denote properties at the transition (or equivalently in the ideal chain state), and

$$\phi = \frac{\langle\phi\rangle}{1-\tilde{\rho}} \quad (2)$$

where  $\tilde{\rho}$  is the occupied volume fraction of the solvent within the volume pervaded by the chain. In general,  $\tilde{\rho}$  is related to its bulk value  $\tilde{\rho}^B$  via equality of chemical potential, leading to the relation:

$$\rho = \tilde{\rho}^B \left( \frac{1-\langle\phi\rangle-\tilde{\rho}}{1-\tilde{\rho}^B} \right)^{r_s} \exp[\beta r_s (\epsilon_{ss}^* (\tilde{\rho}-\tilde{\rho}^B) + 2\epsilon_{sp}^* \langle\phi\rangle)] \quad (3)$$

where  $r_s$  is a solvent size parameter,  $\beta = 1/k_B T$ ,  $s$  and  $p$  subscripts denote solvent and polymer parameters, respectively, and  $\epsilon_{ij}^*$  is an interaction energy parameter between component  $i$  and component  $j$ . The self-interaction energy  $\epsilon_{ii}^*$  of component  $i$  is related to its characteristic temperature as  $T_i^* = \epsilon_{ii}^*/k$ . In the limit of infinite chain length eq 1 is shown to reduce to

$$\tilde{\Theta} = 1 - \tilde{\rho}^B(\Theta) \quad (4)$$

where  $\tilde{\Theta} \equiv \Theta/2T_p^*$ . Equation 4 provides a simple relationship between the equation of state behavior of the solvent and the CGT of the chain.

The mean occupied volume fraction of the chain  $\langle\phi\rangle$  within its pervaded volume is shown to be given by the following equation:

$$\frac{7}{3}(\langle\alpha^2\rangle - 1) = -r\{\beta\epsilon_{pp}^*\langle\phi\rangle + [\ln(1-\phi) + \phi]/\phi\} \quad (5)$$

Here  $\langle\alpha^2\rangle$  is called the chain expansion factor and is defined as the ratio of the mean square gyration radius of the chain to the mean square gyration radius of an ideal chain. It may also be related to the chain occupied volume fraction by

$$\langle\alpha^2\rangle = \frac{a}{r^{1/3}\langle\phi\rangle^{2/3}} \quad (6)$$

where  $a$  is some constant. At a CGT the value of  $\langle\alpha^2\rangle$  is unity.

**2.2. Temperature–Pressure Behavior.** Equations 1, 4, and 5 define only the density–temperature behavior of the chain. In order to consider the effect of pressure on the CGT, an equation of state for the solvent must be introduced. The Sanchez–Lacombe (S–L) lattice fluid model provides such an equation consistent with the derivation of the above theory for the CGT. The S–L bulk solvent density is given by

$$(\tilde{\rho}^B)^2 + \tilde{P}_s + \tilde{T}_s[\ln(1-\tilde{\rho}^B) + (1-1/r_s)\tilde{\rho}^B] = 0 \quad (7)$$

where  $\tilde{P}_s$  and  $\tilde{T}_s$  are reduced temperature and pressure of the solvent and  $r_s$  is the solvent size parameter. Equations 7, 3, and 5 may be solved simultaneously to yield the chain gyration radius or polymer occupied volume fraction as a function of pressure through the CGT.

While the above approach provides a determination of the chain behavior in the vicinity of the CGT, it is also desirable to obtain an equation directly yielding the CGT temperature and pressure. A closed form, analytic equation relating the CGT pressure and temperature of an infinite chain follows from eqs 4 and 7:

$$-\tilde{P}_s = (1-\tilde{\Theta})^2 + 2\tilde{\zeta}\tilde{\Theta}[\ln\tilde{\Theta} + (1-1/r_s)(1-\tilde{\Theta})] \quad (8)$$

where the parameter  $\tilde{\zeta} \equiv T_p^*/T_s^*$  is the ratio of characteristic temperatures of the polymer and solvent and characterizes the relative strength of their self-interactions. Alternatively, for the case of a finite chain, a numerical result for the  $P$ – $T$  behavior of the CGT may be obtained via simultaneous solution of eqs 1, 3, and 7.

As noted in the introduction, an additional value of interest is the slope of the  $P$ – $T$  curve at zero pressure. From eq 8, the slope  $\partial\Theta/\partial P|_{P=0}$  of the CGT for an infinite chain is given by

$$\left. \frac{\partial\Theta}{\partial P} \right|_{P=0} = \frac{T_p^*}{2P_s^*} \left\{ 1 + \tilde{\Theta}_0 \left[ 2\tilde{\zeta} \left( 1 - \frac{1}{r_s} \right) - 1 \right] - \tilde{\zeta} \left( 2 - \frac{1}{r_s} + \ln\tilde{\Theta}_0 \right) \right\}^{-1} \quad (9)$$

where  $\tilde{\Theta}_0 = \tilde{\Theta}|_{P=0}$ . Obtaining a numerical result for eq 9 requires solving eq 8 for temperature at zero pressure and substituting the result into eq 9. For a finite chain  $\partial\Theta/\partial P|_{P=0}$  may be obtained numerical via simultaneous solution of eqs 1, 3, and 7 followed by numerical determination of the slope at  $P = 0$ .

An equation for the temperature of  $P_{max}$  of an infinite chain can be established through a similar approach. From eq 8, this maximum must satisfy the condition

$$\frac{\partial\tilde{P}_s}{\partial\tilde{\Theta}} = 0 = 2 \left\{ 1 + \tilde{\Theta} \left[ 2\tilde{\zeta} \left( 1 - \frac{1}{r_s} \right) - 1 \right] - \tilde{\zeta} \left[ 2 - \frac{1}{r_s} + \ln\tilde{\Theta} \right] \right\} \quad (10)$$

## 3. Results and Discussion

**3.1. Qualitative Predictions.** Typical conformational behavior as predicted by eq 8 is qualitatively consistent with the

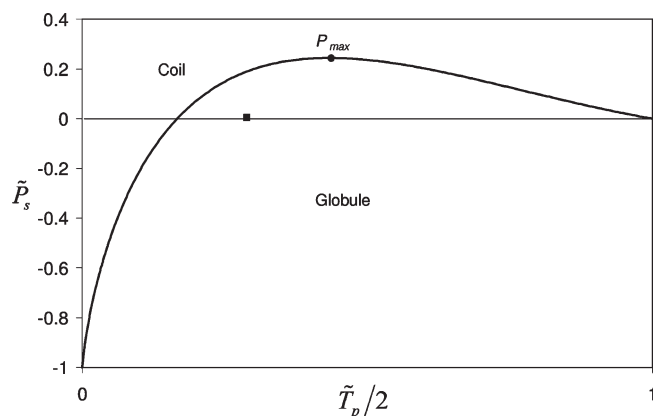


**Figure 2.** Plot of dimensionless CGT pressure versus temperature as predicted by eq 8 for an infinite chain in solution with  $r_s = 10$  and  $\zeta = \tilde{T}_p^*/\tilde{T}_s^* = 2.0$ . Because  $\tilde{\Theta} \equiv \Theta/2\tilde{T}_p^* = (\tilde{T}_p/2)|_{\alpha=1}$ , the scaling of the temperature axis is such that the temperature value given for any point on the curve corresponds to the value of  $\tilde{\Theta}$  at that pressure. The solid square denotes the critical point of the solvent. Values to the left of the hypercritical point  $P_{max}$  correspond to an HCGT while values to the right correspond to a CCGT.

high temperature behavior predicted in the literature, as shown in Figure 1, as well as with predictions of Lennard-Jones simulations for the CGT.<sup>10,11</sup> As shown in Figure 2, it is characterized by an HCGT that smoothly passes into negative pressure at low temperatures, corresponding to a continuation of the chain CGT locus into a region of liquid–vapor metastability for the solvent under tension. At high temperatures, the CGT curves over into a maximum and a high temperature CCGT. Furthermore, for an infinite chain the pressure of the CCGT approaches zero as the system approaches the theoretical vapor–liquid critical temperature of the chain ( $2\tilde{T}_p^*$ ) as calculated via the Sanchez–Lacombe lattice fluid model. For a finite chain, the pressure maximum decreases with decreasing chain length. Furthermore, the temperature at which the high temperature CCGT goes to zero pressure drops and ceases to coincide with the theoretical vapor–liquid critical point of the chain.

**3.2. Quantitative Comparison with Experiment.** Results exhibit a good match with experiment in several quantitative respects. As shown in Figure 3 for PIB in various solvents,  $P$ – $T$  curves predicted from eq 8 for the HCGT at infinite chain length exhibit good agreement with long chain LCST experimental data<sup>4</sup> without the use of any adjustable solution parameters (pure component parameters  $T^*$ ,  $P^*$ ,  $r$ , and  $\rho^*$  for the solvent and polymer are obtained from tabulated Sanchez–Lacombe parameters<sup>35</sup>). Furthermore, theoretical predictions of  $\partial\Theta/\partial P|_{P=0}$ , as shown in Table 1 for a variety of systems, exhibit a generally good match with experimental results, albeit with a moderate bias toward underprediction.

**3.3. Prediction of  $P_{max}$ .** Although eq 10 is not analytically tractable, it is subject to straightforward numerical solution to yield the position of the high pressure hypercritical point. As shown in Figure 4 for long chains, the dimensionless temperature of the pressure maximum  $\tilde{\Theta}_{P_{max}}$  generally decreases with increasing  $\zeta$  and  $r_s$ . This provides a guide to identifying systems offering experimental access to a high temperature UCST because these systems should tend to be characterized by relatively low values of  $\tilde{\Theta}_{P_{max}}$ . Such systems tend to consist of a polymer in a very small molecule solvent such as carbon dioxide, methane, oxygen, nitrogen, or ethylene, as exemplified in Figure 4. Furthermore, as shown in Figure 2,  $P_{max}$  is typically well into the solvent supercritical region. As solutions of polymer in supercritical

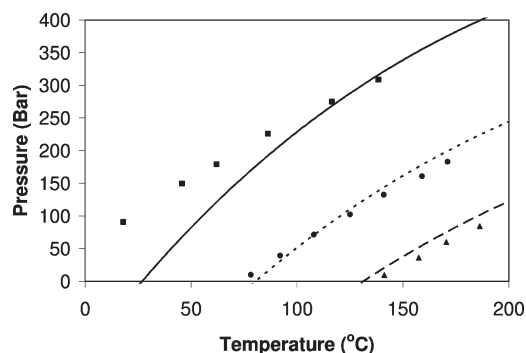


**Figure 3.**  $P$ – $T$  plot of the HCGT of polyisobutylene ( $M_w = 1.66 \times 10^6$  g/mol) in various solvents. Lines correspond to predictions based upon eq 8 for an infinite chain. Points correspond to experimental cloud point data.<sup>4</sup> The solid line and squares correspond to an  $n$ -butane solvent, dotted line and circles to an  $n$ -pentane solvent, and dashed line and triangles to a  $n$ -hexane solvent. The predicted critical points from the Sanchez–Lacombe model for  $n$ -butane,  $n$ -pentane, and  $n$ -hexane are as follows: {161 °C, 44 bar}, {210 °C, 39 bar}, and {253 °C, 36 bar}, respectively.

**Table 1.** Comparison of Theoretical and Experimental Results for  $\partial\Theta/\partial P|_{P=0}$  for Various Systems<sup>a</sup>

polymer	solvent	$\partial\Theta/\partial P _{P=0}$ (°C/bar)	
		experiment	theory
polystyrene	<i>tert</i> -butyl acetate <sup>15</sup>	0.68	0.50
	methyl cyclohexane <sup>14</sup>	0.80	0.65
	methyl acetate <sup>16</sup>	0.47	0.22
polyisobutylene <sup>4</sup>	propane	0.33	0.23
	$n$ -butane	0.37	0.27
	$n$ -pentane	0.45	0.37
	$n$ -hexane	0.61	0.47

<sup>a</sup>Theoretical calculations are based on polymer molecular weights chosen to match those associated with each experimental result.

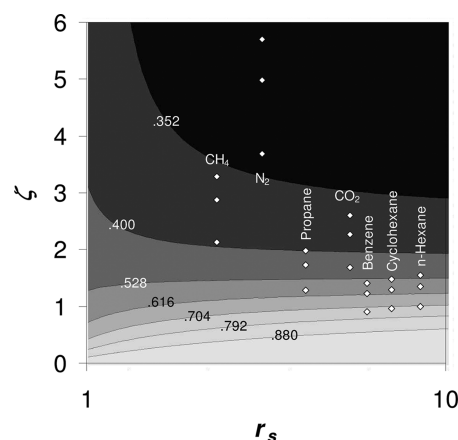


**Figure 4.** Contour plot of temperature  $\tilde{\Theta}_{P_{max}}$  at the high pressure hypercritical point as a function of interaction ratio  $\zeta$  and solvent size  $r_s$  in the limit of infinite chain length. The numbered lines indicate the value of  $\tilde{\Theta}_{P_{max}}$  along that contour. White points indicate the position of various polymer/solvent systems. Each vertical triplet of points corresponds, from top to bottom, to polystyrene, polyisobutylene, and PDMS in the labeled solvent, where these three polymers range from high to low  $T_p^*$  (735, 643, and 476 K, respectively<sup>35</sup>). Note that systems in very small molecule solvents, exemplified here by methane, nitrogen, and carbon dioxide, can provide values of  $\tilde{\Theta}_{P_{max}}$  well below the range of more typical polymer solvents such as propane, benzene, hexane, and cyclohexane.

carbon dioxide are an area of active study, they might provide a convenient system in which to begin a search for a high temperature UCST.



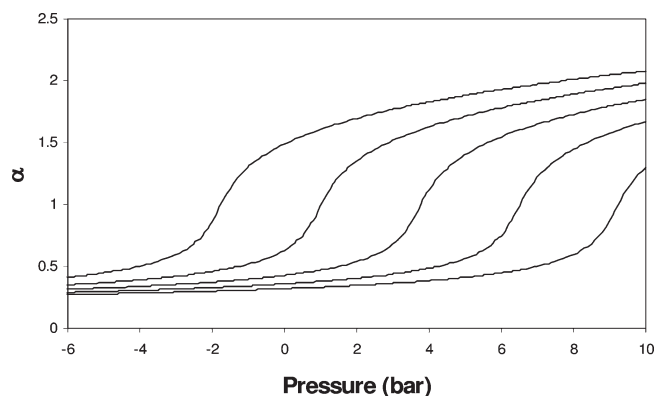


**Figure 5.** Typical plot of chain expansion factor through the pressure induced globule-to-coil transition as predicted by this model, shown as calculated for the system polyisobutylene/*n*-pentane. Curves correspond to different temperatures. From leftmost to rightmost curve, corresponding temperatures are 353, 354, 355, 356, and 357 K.

**3.4. Pressure-Induced Transition.** Whereas the HCGT can be understood as nearly horizontal motion through the CGT locus in Figure 2, a pressure induced coil–globule transition (PGCT) can be understood as vertical motion through the CGT locus. Figure 5 shows typical results for the expansion factor of the chain as a function of pressure through the CGT at temperatures near solvent vapor–liquid equilibrium. The transition is qualitatively similar to experimental results for pressure induced swelling of aqueous polymer networks.<sup>21</sup> As expected, an increase in pressure triggers expansion of the chain. This can be equivalently understood as a pressure induced shift of the CGT temperature upward through the system temperature. In addition, it is apparent that for the small differences in temperature shown in this figure, the  $P$ – $T$  relationship is approximately linear, which is consistent with experimental results over small temperature ranges.

#### 4. Conclusions

The proposed model for single chain pressure/temperature conformational behavior offers semiquantitative agreement with experiment without the use of adjustable parameters. Heating induced coil–globule transition (HCGT) pressures and temperatures associated with the lower critical solution temperature (LCST) transition are well predicted for a variety of polymer/solvent systems, and important qualitative aspects of a polymer phase behavior master curve delineated in the literature are reproduced. Furthermore, predicted values of  $\partial T/\partial P$  of the HCGT at zero pressure ( $\partial T/\partial P|_{P=0}$ ) exhibit reasonable agreement with experimental results.

Qualitatively, predicted behavior is characterized by a heating induced coil-to-globule transition (HCGT) that smoothly passes into negative pressure at low temperatures and curves over into a maximum and a cooling induced coil-to-globule transition (CCGT) at high temperatures. The maximum at which the CCGT and HCGT meet corresponds to a high pressure hypercritical point  $P_{max}$  in the polymer/solvent phase behavior.<sup>2</sup> Although this behavior is experimentally inaccessible in most systems due to polymer degradation, results show that solutions

of polymer in very small molecule solvents may present a  $P_{max}$  at sufficiently low temperatures to allow observation. In particular, polymer/ $\text{CO}_2$  solutions may offer a convenient starting point for a search of such systems for high temperature UCST behavior.

#### References and Notes

- (1) Simmons, D.; Sanchez, I. C. *Macromolecules* **2008**, *41*, 5885–5889.
- (2) Imre, A. R.; Melnichenko, G.; Hook, W. A. V. *Phys. Chem. Chem. Phys.* **1999**, *1*, 4287–4292.
- (3) Konynenburg, P. H. C.; Scott, R. L. *Philos. Trans. R. Soc. London, Ser. A, Math. Phys. Sci.* **1980**, 298 (1442), 495–540.
- (4) Zeman, L.; Biros, J.; Delmas, G.; Patterson, D. J. *Phys. Chem.* **1972**, *76*, 1206–1213.
- (5) Imre, A. R.; Hook, W. A. V.; Wolf, B. A. *Macromol. Symp.* **2002**, *181*, 363–372.
- (6) Lacombe, R. H.; Sanchez, I. C. *J. Phys. Chem.* **1976**, *80*, 2568–2580.
- (7) Folie, B.; Radosz, M. *Ind. Eng. Chem. Res.* **1995**, *34*, 1501–1516.
- (8) Schneider, G. M. *Phys. Chem. Chem. Phys.* **2002**, *4*, 845–852.
- (9) Leder, D.; Irani, C. A. *J. Chem. Eng. Data* **1975**, *20*, 3.
- (10) Luna-Barcenas, G.; Gromov, D. G.; Meredith, J. C.; Sanchez, I. C.; Pablo, J. J. d.; Johnston, K. P. *Chem. Phys. Lett.* **1997**, *278*, 302–306.
- (11) Luna-Barcenas, G.; Meredith, J. C.; Sanchez, I. C.; Johnston, K. P.; Gromov, D. G.; Pablo, J. J. d. *J. Chem. Phys.* **1997**, *107*, 10782–10792.
- (12) Lu, X.; Korgel, B. A.; Johnston, K. P. *Nanotechnology* **2005**, *16*, 389–394.
- (13) Loos, T. W. d.; Poot, W.; Diepen, G. A. M. *Macromolecules* **1983**, *16*, 111–117.
- (14) Enders, S.; Loos, T. W. d. *Fluid Phase Equilib.* **1997**, *139*, 335–347.
- (15) Saeki, S.; Kuwahara, N.; Kaneko, M. *Macromolecules* **1976**, *9*, 101–106.
- (16) Zeman, L.; Patterson, D. J. *Phys. Chem.* **1972**, *76*, 1214–1219.
- (17) Bekiranov, S.; Bruinsma, R.; Pincus, P. *Phys. Rev. E* **1997**, *55*, 577–585.
- (18) Cook, R. L.; H. E. King, J.; Peiffer, D. G. *Phys. Rev. Lett.* **1992**, *69*, 3072–3075.
- (19) Karlstrom, G. J. *Phys. Chem.* **1985**, *89*, 4962–4964.
- (20) Nasimova, I.; Karino, T.; Okabe, S.; Nagao, M.; Shibayam, M. *J. Chem. Phys.* **2004**, *121*, 9708–9715.
- (21) Zhong, X.; Wang, Y. X.; Wang, S. C. *Chem. Eng. Sci.* **1996**, *51*, 3235–3239.
- (22) Kubota, K.; Fujishige, S. *J. Phys. Chem.* **1990**, *94*, 5154–5158.
- (23) Gao, J.; Wu, C. *Macromolecules* **1997**, *30*, 6873–6876.
- (24) Xhang, X. Z.; Zhou, R. X.; Cui, J. Z.; Zhang, J. T. *Int. J. Pharm.* **2002**, *235*, 43–50.
- (25) Joeong, B.; Kim, S. W.; Bae, Y. H. *Adv. Drug Delivery Rev.* **2002**, *54*, 37–51.
- (26) Ballauff, M.; Lu, Y. *Polymer* **2007**, *48*, 1815–1823.
- (27) Akasaka, K.; Tezuka, T.; Yamada, H. *J. Mol. Biol.* **1997**, *271*, 671–678.
- (28) Hayakawa, I.; Linko, Y.; Link, P. *Lebensm. Wiss. Technol.* **1996**, *29*, 756–762.
- (29) Kunugi, S.; Tanaka, N. *Biochim. Biophys. Acta* **2002**, *1595*, 329–344.
- (30) Lang, D. *J. Mol. Biol.* **1973**, *78*.
- (31) Lang, D.; Taylor, T. N.; Dobyan, D. C.; Gray, D. M. *J. Mol. Biol.* **1976**, *106* (1), 97–107.
- (32) Vasilevskaya, V. V.; Khokhlov, A. R.; Matsuzawa, Y.; Yoshikawa, K. *J. Chem. Phys.* **1995**, *102* (16), 6595–6602.
- (33) Melnikov, S. M.; Sergeyev, V. G.; Yoshikawa, K. *J. Am. Chem. Soc.* **1995**, *117* (40), 9951–9956.
- (34) Dias, R. S.; Innerlohinger, J.; Glatter, O.; Miguel, M. G.; Lindman, B. *J. Phys. Chem. B* **2005**, *109*, 10458–10463.
- (35) Sanchez, I. C.; Stone, M. In *Polymer Blends*; Paul, D. R., Bucknall, C. B., Eds.; John Wiley & Sons, Inc.: New York, 2000; Vol. 1, p 51.